

# **Characterization of Stress-Exposed Granulocyte Colony Stimulating Factor Using ELISA and Hydrogen/Deuterium Exchange Mass Spectrometry**

Daisuke Tsuchida<sup>1, 2\*</sup>, Katsuyoshi Yamazaki<sup>1</sup>, Satoko Akashi<sup>2\*</sup>

1: Bio Process Research and Development Laboratories, Kyowa Hakko Kirin Co., Ltd.,  
Takasaki, Gunma 370-0013, Japan

2: Graduate School of Medical Life Science, Yokohama City University, Yokohama,  
Kanagawa 230-0045, Japan

Running Title: HDX-MS of stress-exposed G-CSF

Key Words: HDX-MS, G-CSF, Receptor-binding activity, Conformation

\* Correspondence to : Daisuke Tsuchida or Satoko Akashi

Daisuke Tsuchida

Bio Process Research and Development Laboratories, Kyowa Hakko Kirin Co., Ltd.

E-mail: [daisuke.tsuchida@kyowa-kirin.co.jp](mailto:daisuke.tsuchida@kyowa-kirin.co.jp)

Tel: +81-27-353-7084, Fax: +81-27-352-4977

100-1 Hagiwara-machi, Takasaki, Gunma 370-0013, Japan

Satoko Akashi

Yokohama City University

E-mail: [akashi@tsurumi.yokohama-cu.ac.jp](mailto:akashi@tsurumi.yokohama-cu.ac.jp)

Tel: +81-45-508-7217, Fax: +81-45-508-7362

1-7-29 Suehiro-cho, Tsurumi-ku, Yokohama, Kanagawa 230-0045, Japan

## Abstract

Information on the higher-order structure is important in the development of biopharmaceutical drugs. Recently, hydrogen/deuterium exchange coupled with mass spectrometry (HDX-MS) has been widely used as a tool to evaluate protein conformation, and unique automated systems for HDX-MS are now commercially available. To investigate the potential of this technique for the prediction of the activity of biopharmaceuticals, granulocyte colony stimulating factor (G-CSF), which had been subjected to three different stress types, was analyzed using HDX-MS and through comparison with receptor-binding activity. It was found that HDX-MS in combination with ion mobility separation was able to identify conformational changes in G-CSF induced by stress, and a good correlation with the receptor-binding activity was demonstrated, which cannot be completely determined by conventional peptide mapping alone. The direct evaluation of biological activity using bioassay is absolutely imperative in biopharmaceutical development, but HDX-MS can provide the alternative information in a short time on the extent and location of the structural damage caused by stresses. Furthermore, the present study suggests the possibility of this system being a versatile evaluation method for the preservation stability of biopharmaceuticals.

## Introduction

In the development of biopharmaceutical products, information on their higher-order structure is considered to be necessary in various situations such as comparability studies when changing manufacturing sites, investigations on unknown biological activity decline, and so on [1]. The US Food and Drug Administration (FDA) released a draft guidance for biosimilar drug development in 2012 [2], stating that structural information on a protein, not just the primary structure but also the higher-order structure, is important for its biological function. As such, an appropriate analytical method is required to evaluate the integrity of the protein structure. To characterize the higher-order structure of a protein with high resolution, X-ray crystallography and nuclear magnetic resonance (NMR) are now used as versatile tools. However, limitations remain in using these techniques for the high-throughput evaluation of biopharmaceuticals; X-ray crystallography requires crystallization of the protein, while application of NMR to large proteins (>30 kDa) is not practical. Furthermore, it is not easy to obtain structural information on heterogeneous mixtures of proteins with a small sample volume.

Recently, hydrogen/deuterium exchange mass spectrometry (HDX-MS) has been recognized as a general tool for characterizing protein conformation. This technique cannot provide the three-dimensional structure of a protein with high resolution at the atomic level, but can detect changes in structure with peptide-length (3-25 amino acids) resolution [3]. The key advantages are that the technique requires only a small amount of the sample, a large molecular size is acceptable, and the analysis can be completed within a relatively short time.

With this technique, amide hydrogen atoms on the protein backbone are easily replaced with deuterium under deuterium-rich conditions, if they are located on the protein surface and are not involved in hydrogen bonding [4]. The rate of deuterium exchange depends on the microenvironment around the particular amide hydrogen, as well as the solution pH and temperature. The amide hydrogens that are in folded conformation cannot easily be substituted with deuterium, and the exchange rate is reduced in the solution at low pH or low temperature [5-7]. Since mass spectrometry can accurately determine the exact mass of a protein, it is easy to determine deuterium intake into the protein. At present, many applications of this technique, measuring the deuterium uptake at digested peptide levels to biopharmaceutical drug development have been reported, including conformational dynamics of antibodies (global HDX analysis, too) [8], epitope mapping of antibodies [9, 10], protein-ligand interactions [11], and characterization of antibody aggregates [12].

In the present study, characterization of stress-exposed G-CSF, a major biopharmaceutical drug for neutropenia, was carried out. The three-dimensional structure of G-CSF has already been determined using X-ray crystallography [13, 14] and NMR [15], and the receptor recognition sites of G-CSF have also been elucidated [16-19] [PDB code 2D9Q]. So far, the effects of methionine oxidation on biological activity [20], and the conformational change by PEGylation to the N-terminal methionine [21], have been investigated for this protein. In this study, G-CSF was exposed to three types of stress: heating, photoirradiation, and oxidation. The resulting changes in structure and biological activity were analyzed using HDX-MS, ion mobility mass spectrometry (IM-MS), and enzyme-linked immunosorbent assay (ELISA). We

discuss here the relationship between the structural change and biological activity of G-CSF, and the potential of HDX-MS as a high-throughput evaluation tool for activity in biopharmaceutical drug development.

## Experimental

### *Sample Preparation*

G-CSF (Filgrastim BS 150 µg Syringe for Inj. MOCHIDA; Mochida Pharm. Co., Ltd, Tokyo, Japan) in the original formulation buffer [sodium acetate (undisclosed concentration), 5% D-mannitol (w/v), 0.04 mg/mL polysorbate 80 at pH 4.0] was degraded in three ways: heat degradation (HD), photo degradation (PD) and forced oxidation (FO). In HD, the protein was incubated at 50°C for a month and underwent size-exclusion chromatography (SEC, see below for details) to isolate the main peak in order to remove aggregated species. In PD, based on the information given in the ICH guidelines [22], the protein was exposed to white fluorescent light over 1.2 million lux hours, as well as integrated near ultraviolet energy over 200 watt hours/square meter. The FO sample was prepared by the addition of 30% hydrogen peroxide (Wako Pure Chemical Industries, Ltd., Osaka, Japan) to the protein solution to give a final concentration of 1%, and the resulting solution was incubated at 25°C for 24 h. As a final step, the solvent of the non-stressed (NS) and all the degraded proteins was exchanged to 10 mM sodium acetate with 5% D-mannitol (w/v) at pH 4.0, and the protein concentration was adjusted to ca. 1 mg/mL (53 µM) using an ultrafiltration device (Amicon-Ultra; Millipore Corporation, Billerica, MA, USA).

### *Size-Exclusion Chromatography (SEC)*

SEC was performed to evaluate the sample purity in terms of molecular size. A 10 µg aliquot of each sample was loaded onto a size-exclusion column (TSKgel G3000SW<sub>XL</sub>; Tosoh

Corporation, Tokyo, Japan) on an HPLC system (Agilent 1200 series; Agilent Technologies, Santa Clara, CA, USA). Separation was achieved with a solvent of 0.1 M sodium phosphate (Wako) and 0.15 M sodium chloride (Wako) at pH 2.5, at a flow rate of 1 mL/min, and monitored by a UV detector at 215 nm. To avoid non-specific adsorption, 2 mg/mL bovine serum albumin was injected before each sample injection [23, 24].

### *Peptide Mapping*

Sites modified by the applied stress were determined by peptide mapping with HPLC-UV detection. A 50 µg aliquot of each sample was reconstituted in a denaturing solvent [5 M urea (MP Biomedicals, LLC., Santa Ana, CA, USA), 0.2 M tris (hydroxymethyl) aminomethane hydrochloride (Nacalai Tesque, Inc., Kyoto, Japan), 0.04 M methylamine hydrochloride (Sigma-Aldrich Corporation, St. Louis, MO, USA), 0.02 M dithiothreitol (Sigma-Aldrich)]. Digestion with Endoproteinase Glu-C (Roche Diagnostics, Indianapolis, IN, USA) was performed with an enzyme to substrate ratio of 1:25 at 25°C for 18 h. The digested samples were separated with a reversed-phase column (VYDAC C4 214TP52, 2.1 mm × 250 mm, 5 µm particle diameter; Alltech Associates, Inc., Deerfield, IL, USA) by a gradient elution of solvent A [0.1% trifluoroacetic acid (HPLC grade; Wako)] and solvent B [90% acetonitrile (HPLC grade; Wako) / 10% water / 0.1% trifluoroacetic acid] on a UPLC system (Waters Corporation, Milford, MA, USA). Peptides were eluted by the following gradient program: 2% B (2 min), 2%–30% B (28 min), 30%–50% B (55 min) and 50%–98% B (5 min), at a flow rate of 0.2 mL/min and detected by UV at 214 nm [25]. Mass information was collected

using a quadrupole time-of-flight mass spectrometer (SYNAPT G2 HDMS; Waters) in the MS<sup>E</sup> mode.

#### *Enzyme-Linked Immunosorbent Assay (ELISA)*

ELISA was performed to assess the receptor binding activity of samples. An appropriate amount of each sample was mixed with a blocking solution [2 mg/mL I-Block (Applied Biosystems, Carlsbad, CA, USA) in PBS], resulting in G-CSF concentrations of 400, 80, 16, 3.2, 0.64, 0.128, and 0.0256 ng/mL. These solutions were then introduced into each well in the 96-well microplate solid-phased with G-CSF receptor (Recombinant Human GCSFR/Fc Chimera; Sino Biological Inc., Beijing, China). After incubation at room temperature, anti-human G-CSF antibody (Human G-CSF Biotinylated Antibody; R&D Systems Inc., Minneapolis, MN, USA) and avidin-labeled peroxidase (Pierce, Thermo Scientific, Rockford, IL, USA) were added, and reacted with the peroxidase substrate (TMB Microwell Peroxidase Substrate System; KPL Inc., Gaithersburg, MD, USA). Receptor binding activity could be determined by the absorbance at 450 nm using a microplate reader. The assays were carried out three times and the average was calculated.

#### *Ion Mobility Mass Spectrometry (IM-MS)*

IM-MS was performed to investigate the molecular size distribution in the gas phase. Samples reconstituted in 10 mM ammonium acetate at pH 4.0 were subjected to analysis with SYNAPT G2 HDMS using metal-coated borosilicate glass capillaries (nanoflow probe tips



thin walled; Waters). Each experimental parameter was set as follows: ESI capillary voltage 0.8 kV, source temperature 50°C, sampling cone voltage 40 V, IMS wave velocity 740 m/s, and IMS wave height 40 V. The data were acquired at  $m/z$  500–4000 every 1 s, and accumulated for 10 min.

#### *H/D Exchange Mass Spectrometry (HDX-MS)*

HDX-MS was performed to evaluate the higher-order protein structure in solution. An automated HDX System (Waters) coupled with SYNAPT G2 HDMS was used in all experiments. Each sample was diluted 20-fold by a blank solution [10 mM sodium acetate (Wako) at pH 4.0] or a deuterated solution [10 mM sodium acetate in D<sub>2</sub>O (Sigma-Aldrich) at pD 4.0 (pD = pH<sub>read</sub> + 0.40) [26, 27]]. The samples were then incubated for 0 s (blank, no deuteration), 10 s, 1, 12, 60, and 240 min (deuteration) at 25°C, and subsequently quenched by mixing with an equal volume of the quench solution [200 mM sodium acetate, 1.5 M guanidine hydrochloride (MP Biomedicals), 0.5 M tris(2-carboxyethyl)phosphine (Pierce)] [21] at 4°C. The quenched samples were then loaded onto an online pepsin-digestion column (immobilized pepsin column, 2.1 mm × 30 mm; Applied Biosystems), in which the digestion and peptide trapping were performed for 4 min at 20°C at pH 2.5 (pH adjusted by formic acid), and the peptides were eluted at a flow rate of 250 µL/min. The digested peptides were then introduced to a UPLC column (ACQUITY UPLC BEH C18, 1.0 mm × 100 mm, 1.7 µm particle diameter; Waters) at 0°C. The peptides were separated with a gradient elution of solvent A (0.1% formic acid) and solvent B (0.1% formic acid in acetonitrile) [8%–40% B (6

min), 40%–90% B (0.5 min) and 90% B (1.5 min)] at a flow rate of 30  $\mu$ L/min. The ion mobility function was also utilized to effectively separate the peptides. The IMS wave velocity and IMS wave height were set at 650 m/s and 40 V, respectively. The extent of back-exchange was regarded as around 30% from the analysis of highly deuterated peptide standard. Because all the experiments were performed under identical condition, the correction of deuterium level was not implemented as described elsewhere [6, 28]. Based on the three independent repetitive experiments (different days) of the NS sample, the standard deviation (SD) of deuterium uptake levels at each labeling time point and their sum of at all labeling time points were  $\pm 0.17$  Da and  $\pm 0.48$  Da respectively, which are similar to the previously reported values [21, 28]. The values of 3 SD (i.e.,  $\pm 0.5$  Da), for each labeling time point and  $\pm 1.4$  Da for the sum of the levels at all labeling time points, were considered as appropriate criteria to judge significant difference.

The peptic peptides of undeuterated protein were identified by the analytical software, ProteinLynx Global SERVER (Waters). Then, all the data including deuterated samples were processed with another analytical software, DynamX (Waters). The experiments were performed in triplicate.

## Results and Discussion

### *Peptide Mapping of Stress-Exposed G-CSF Monomer*

To identify the exact characteristics of the G-CSF monomer, impurities in the samples, such as artificial aggregates, are undesirable. Under the HD condition, the amount of artificial aggregates increased depending on the storage time, so they were removed by SEC fractionation, and the major peak corresponding to the G-CSF monomer was isolated. Because no significant impurity was recognized in the SEC chromatograms of the other samples (NS, PD, and FO), the fractionation process was skipped for them. Figure 1 shows the SEC chromatograms of the NS, fractionated HD, PD, and FO samples. Only a single peak appeared at the same retention time, suggesting that all four samples have an identical purity profile and that impurities of a different size do not exist in the sample.

Next, peptide mapping was performed to characterize the modification in each degraded G-CSF (Figure 2). The NS, HD, and PD samples exhibited similar chromatograms, demonstrating that heat and photo stresses do not cause any modification to the protein. In contrast, three peaks (marked as a, b, and c) disappeared, while three novel peaks (a\*, b\*, and c\*) appeared in the FO sample. Using LC/MS<sup>E</sup> analysis, these peaks were revealed to contain oxidized methionine residues: Met<sup>127</sup> and Met<sup>138</sup> in peak a\* (Leu<sup>125</sup>–Glu<sup>163</sup>), Met<sup>1</sup> in peak b\* (Met<sup>1</sup>–Glu<sup>20</sup>), and Met<sup>122</sup> in peak c\* (Leu<sup>100</sup>–Glu<sup>124</sup>), as summarized in Table 1. No other modification was detected in the FO sample. This is consistent with previously reported data [20].

### *ELISA of Stress-Exposed G-CSF Monomer*

To assess the receptor binding activity, ELISA was performed for each sample in triplicate. In this experiment, the absorbance at 450 nm reflects the level of interaction between the sample proteins and the G-CSF receptor. The results are summarized in Table 2. Relative receptor binding activity was calculated against the original G-CSF drug product (reference material). Considering the SD value of this ELISA experiment (ca. 4.5%, data not shown), and the dispersion of the measured values, the receptor binding activity of the HD and PD samples are considered to be almost identical (83%–89%) to the NS sample, whereas the FO sample showed a significant decrease (46%). The results suggest that oxidation stress might have contributed to the decline in the receptor binding activity of the FO sample, whereas other stresses had little effect.

### *IM-MS of Stress-Exposed G-CSF Monomer*

To characterize the higher-order structure of the stress-exposed samples, IM-MS was performed and the collision cross-section distribution in the gas phase was obtained. In the present study, we carried out ESI-IM-MS analysis of the samples in 10 mM ammonium acetate solution at pH 4.0, which is similar to the original solvent of the drug product [sodium acetate (undisclosed concentration, pH 4.0), 5% D-mannitol (w/v), 0.04 mg/mL polysorbate 80]. In the mass spectra of the four G-CSF samples, multiply charged ions with 6+ through 19+ were observed, as shown in Figure 3a.

The most intense peak (8+) was picked up, and its driftgram was plotted (Figure 3b). The drift time of the stress-exposed samples, especially FO, shifted slightly to a later time, which suggests that the stress-exposed G-CSF structure was relaxed to some extent. As the resolution of ion mobility separation is not very high, a substantial change in the structure is needed to clearly separate protein ions using ion mobility spectrometry, especially for large proteins. A slight change in the driftgram would thus imply that the conformational changes of the degraded samples are insignificant.

#### *HDX-MS of Stress-Exposed G-CSF Monomer*

For further investigation into the conformation of the stress-exposed G-CSF, HDX-MS was performed. First, experimental conditions were optimized in order to achieve a high score in the sequence coverage. By simple LC/MS<sup>E</sup> analysis of peptic peptides, the score of the sequence coverage achieved was less than 90% (data not shown), which is not high enough to extensively investigate the complete protein conformation. This might be due to the steep LC gradient, which allows for rapid elution of peptides to avoid back-exchange of the amide hydrogens. It proved difficult to resolve the peptides well using the short-time elution. To accomplish a high resolution of the peptides with an identical LC gradient, IMS separation was added to the measurement scheme of LC/MS<sup>E</sup>. When MS<sup>E</sup> measurement was performed in combination with IMS separation, co-eluting peptides in the LC chromatogram could be separated by an additional dimension, drift time, which resulted in accurate identification of peptic fragments and improved sequence coverage [29]. It was found that the observed

peptides covered all receptor recognition sites, including site II (major: residues Lys<sup>17</sup>-Lys<sup>24</sup> and Leu<sup>109</sup>-Asp<sup>113</sup>) and site III (minor: residues Tyr<sup>40</sup>-Ser<sup>54</sup> and Phe<sup>145</sup>-Arg<sup>148</sup>) (Figure 4) [19] [PDB code 2D9Q]. The supplemental use of IMS improved the sequence coverage up to 97%, as shown in Figure 4. MS<sup>E</sup> experiments in combination with IMS were carried out two more times, and high scores of sequence coverage (91% and 93%) were reproducibly obtained.

Next, HDX-MS was performed on the NS, HD, PD and FO samples. Supplementary Figure S-1 shows deuterium uptake curves for the peptides derived from these samples. The observed mass difference of each peptic peptide between the NS and stress-exposed G-CSF was analyzed in detail. Figure 5 shows a summary of the results for the first trial of HDX-MS. The x-axis shows the observed peptide, and the y-axis shows the mass difference calculated by subtraction of the observed mass of stress-exposed G-CSF from that of NS. The vertical black bar shows the sum of the mass difference at each time point. In the difference chart of the NS versus HD sample (Figure 5a), the color plots and vertical bars converged at the center line (at 0.0) and the mass differences for almost all of the peptides were insignificant (significance criteria are  $\pm 0.5$  Da for the color plots and  $\pm 1.4$  Da for the vertical bars, as mentioned in the Experimental section), which means that no significant change in their higher-order structure was recognized by HDX analysis. The difference chart of the NS versus PD sample (Figure 5b) demonstrates that deuterium uptake in the NS and PD samples are similar, but all the plots and bars are on the PD side. This may suggest that photoirradiation induced a slight relaxation in the protein structure. However, considering the significance criteria, the difference in deuterium uptake between the NS and PD samples can

be regarded as insignificant and can be ignored. In contrast, in the case of the FO sample, significant differences were observed in a broad range of the sequence in the difference chart (Figure 5c). Supplementary Figure S-2 and S-3 show typical mass spectra for the peptides at each time point; peptide 93-104 did not show a significant difference in deuterium uptake between the NS and FO samples, whereas peptide 162-175 presented a considerable difference between the two samples. In particular, the N- and C-terminal regions including receptor recognition sites show a large negative extension in the vertical bars, implying that the FO sample has a more extended structure than the NS sample, resulting in high deuterium intake. Since the peptides that cover the receptor recognition site II exhibit large negative values in their relative fractional uptake scores, it is likely that conformational changes occurred mainly around site II. In addition, the C-terminal region from Ala<sup>142</sup> through Pro<sup>175</sup> showed a big increase in deuterium uptake, suggesting that a drastic structural change also occurred in this region. Considering that ELISA showed a significant drop in receptor binding activity for the FO sample, a considerable degree of structural change in these regions is likely to have caused the large reduction in activity.

Peptide mapping of the FO sample determined that four methionine residues were specifically oxidized, and its ELISA revealed a significant drop in the receptor binding activity. Since the four identified oxidized methionine residues are not located on the receptor recognition sites [19], the structure-activity relationship cannot be fully revealed using only sequence analysis and ELISA. In contrast, HDX-MS of the FO sample showed a drastic increase in deuterium uptake in a rather broad region, including the receptor binding sites. All four methionine

residues were included in the peptides that showed an increase in deuterium uptake. In a previous paper, chemical modification and site-directed mutagenesis were carried out to determine the order of methionine oxidation ( $\text{Met}^1 > \text{Met}^{138} > \text{Met}^{127} \gg \text{Met}^{122}$ ) and to correlate the effects of oxidation on the stability and biological activity of G-CSF [20]. However, in the present study, it was possible and quite easy to investigate the relationship between the conformational changes and receptor-binding activity using HDX-MS. As demonstrated here, HDX-MS is a promising tool for obtaining structural information on biopharmaceuticals within a short time in order to verify their biological activity.



## Conclusions

In this study, three kinds of degraded samples were prepared and assessed using various analytical techniques. SEC and peptide mapping demonstrated that the samples have an identical purity profile and primary structure, except for methionine oxidation in the FO sample. ELISA data showed a decrease in receptor binding activity for the FO sample, but IM-MS could not significantly detect this aspect. On the contrary, HDX-MS could sensitively detect the change in the higher-order structure, and showed a good correlation with receptor binding activity for the stress-exposed samples.

In the development of biopharmaceutical products, the importance of higher-order structure evaluation increases every year. In this study, we found that HDX-MS is a promising tool for detecting conformation changes in G-CSF, and can easily provide the information on the structural damage by stress. This technique is also quite advantageous in that only a small amount of sample and a short time are required for analysis. Further studies may be required, but HDX-MS shows great potential as an indispensable tool in the biopharmaceutical drug development.

## Acknowledgment

The authors acknowledge partial support for this work by a grant for academic research from Yokohama City University (to S.A.).

The final publication is available at Springer via <http://dx.doi.org/10.1007/s13361-014-0959-z>.

## References

1. Scapin, G.: Structural biology and drug discovery. *Curr. Pharm. Des.* 12, 2087-2097 (2006)
2. Guidance for Industry Quality Considerations in Demonstrating Biosimilarity to a Reference Protein Product. *DRAFT GUIDANCE*, FDA (2012)
3. Zhang, Z., Smith, D.L.: Determination of amide hydrogen exchange by mass spectrometry: a new tool for protein structure elucidation. *Protein Sci.* 2, 522-531 (1993)
4. Engen, J.R., Wales, T.E., Shi, X.: Hydrogen exchange mass spectrometry for conformational analysis of proteins. *Encycl. Anal. Chem. Wiley*, 2-17 (2011)
5. Hoofnagle, A.N., Resing, K.A., Ahn, N.G.: Protein analysis by hydrogen exchange mass spectrometry. *Annu. Rev. Biophys. Biomol. Struct.* 32, 1-25 (2003)
6. Wales, T.E., Engen, J.R.: Hydrogen exchange mass spectrometry for the analysis of protein dynamics. *Mass Spectrom. Rev.* 25, 158-170 (2006)
7. Woodward, C., Simon, I., Tüchsen, E.: Hydrogen exchange and the dynamic structure of proteins. *Mol. Cell. Biochem.* 48, 135-160 (1982)
8. Houde, D., Arndt, J., Domeier, W., Berkowitz, S., Engen, J.R.: Characterization of IgG1 conformation and conformational dynamics by hydrogen/deuterium exchange mass spectrometry. *Anal. Chem.* 81, 2644-2651 (2009)
9. Zhang, Q., Willison, L.N., Tripathi, P., Sathe, S.K., Roux, K.H., Emmett, M.R., Blakney, G.T., Zhang, H.M., Marshall, A.G.: Epitope mapping of a 95 kDa antigen in complex with antibody by solution-phase amide backbone hydrogen/deuterium exchange

- monitored by Fourier transform ion cyclotron resonance mass spectrometry. *Anal. Chem.* 83, 7129–7136 (2011)
10. Obungu, V.H., Gelfanova, V., Rathnachalam, R., Bailey, A., Sloan-Lancaster, J., Huang, L.: Determination of the mechanism of action of anti-FasL antibody by epitope mapping and homology modeling. *Biochemistry* 48, 7251–7260 (2009)
  11. Chalmers, M.J., Busby, S.A., Pascal, B.D., He, Y., Hendrickson, C.L., Marshall, A.G., Griffin, P.R.: Probing protein ligand interactions by automated hydrogen/deuterium exchange mass spectrometry. *Anal. Chem.* 78, 1005–1014 (2006)
  12. Zhang, A., Singh, S.K., Shirts, M.R., Kumar, S., Fernandez, E.J.: Distinct aggregation mechanisms of monoclonal antibody under thermal and freeze-thaw stresses revealed by hydrogen exchange. *Pharm. Res.* 29, 236-250 (2012)
  13. Hill, C.P., Osslund, T.D., Eisenberg, D.: The structure of granulocyte-colony-stimulating factor and its relationship to other growth factors. *Proc. Natl. Acad. Sci. U.S.A.* 90, 5167-5171 (1993)
  14. Aritomi, M., Kunishima, N., Okamoto, T., Kuroki, R., Ota, Y., Morikawa, K.: Atomic structure of the GCSF-receptor complex showing a new cytokine-receptor recognition scheme. *Nature* 401, 713-717 (1999)
  15. Zink, T., Ross, A., Lüers, K., Cieslar, C., Rudolph, R., Holak, T.A.: Structure and dynamics of the human granulocyte-colony stimulating factor determined by NMR spectroscopy. Loop mobility in a four-helix-bundle protein. *Biochemistry* 33, 8453-8463 (1994)

16. Reidhaar-Olson, J.F., De Souza-Hart, J.A., Selick, H.E.: Identification of residues critical to the activity of human granulocyte colony-stimulating factor. *Biochemistry* 35, 9034-9041 (1996)
17. Young, D.C., Zhan, H., Cheng, Q.L., Hou, J., Matthews, D.J.: Characterization of the receptor binding determinants of granulocyte colony stimulating factor. *Protein Sci.* 6, 1228-1236 (1997)
18. Layton, J.E., Shimamoto, G., Osslund, T., Hammacher, A., Smith, D.K., Treutlein, H.R., Boone, T.: Interaction of granulocyte colony-stimulating factor (G-CSF) with its receptor. Evidence that Glu<sup>19</sup> of G-CSF interacts with Arg<sup>288</sup> of the receptor. *J. Biol. Chem.* 274, 17445–17451 (1999)
19. Tamada, T., Honjo, E., Maeda, Y., Okamoto, T., Ishibashi, M., Tokunaga, M., Kuroki, R.: Homodimeric cross-over structure of the human granulocyte colony-stimulating factor (GCSF) receptor signaling complex. *Proc. Natl. Acad. Sci. U.S.A.* 103, 3135-3140 (2006)
20. Lu, H.S., Fausset, P.R., Narhi, L.O., Horan, T., Shinagawa, K., Shimamoto, G., Boone, T.C.: Chemical modification and site-directed mutagenesis of methionine residues in recombinant human granulocyte colony-stimulating factor: effect on stability and biological activity. *Arch Biochem. Biophys.* 362(1), 1-11 (1999)
21. Wei, H., Ahn, J., Yu, Y.Q., Tymiak, A., Engen, J.R.: Using hydrogen/deuterium exchange mass spectrometry to study conformational changes in granulocyte colony stimulating factor upon PEGylation. *J. Am. Soc. Mass Spectrom.* 23, 498-504 (2012)

22. ICH Harmonised Tripartite Guideline, Stability Testing: Photostability Testing of New Drug Substances and Products, ICH (1996)
23. Dalmore, S.L., D'Avila, F.B., da Silva, L.M., Bergamo, A.C., Zimmermann, E.S.: Development and validation of a capillary zone electrophoresis method for assessment of recombinant human granulocyte colony-stimulating factor in pharmaceutical formulations and its correlation with liquid chromatography methods and bioassay. *J. Chromatogr. B* 877, 2471-2476 (2009)
24. Skrlin, A., Radic, I., Vuletic, M., Schwinke, D., Runac, D., Kusalic, T., Paskvan, I., Krsic, M., Bratos, M., Marinc, S.: Comparison of the physicochemical properties of a biosimilar filgrastim with those of reference filgrastim. *Biologicals* 38, 557-566 (2010)
25. The Japanese Pharmacopeia, 16th ed. Supplement 1, Ministry of Health, Labour and Welfare, Japan (2012)
26. Glasoe, P.K., Long, F.A.: Use of glass electrodes to measure acidities in deuterium oxide. *J. Phys. Chem.* 64, 188-189 (1960)
27. Connelly, G.P., Bai, Y., Jeng, M.F., Englander, S.W.: Isotope effects in peptide group hydrogen exchange. *Proteins* 17, 87-92 (1993)
28. Iacob, R.E., Bou-Assaf, G.M., Makowski, L., Engen, J.R., Berkowitz, S.A., Houde, D.: Investigating monoclonal antibody aggregation using a combination of H/DX-MS and other biophysical measurements. *J. Pharm. Sci.* 102, 4315-4329 (2013)

29. Iacob, R.E., Murphy, J.P., Engen, J.R.: Ion mobility adds an additional dimension to mass spectrometric analysis of solution-phase hydrogen/deuterium exchange. *Rapid Commun. Mass Spectrom.* 22, 2898-2904 (2008)
30. Kavan, D., Man, P.: MStools - Web based application for visualization and presentation of HXMS data. *Int. J. Mass Spectrom.* 302, 53-58 (2011)

**Table 1.** Glu-C Peptides with Methionine Residues

Peak	Sequence	Oxidized methionines
a	Leu <sup>125</sup> –Glu <sup>163</sup>	
a*	Leu <sup>125</sup> –Glu <sup>163</sup>	Met <sup>127</sup> , Met <sup>138</sup>
b	Met <sup>1</sup> –Glu <sup>20</sup>	
b*	Met <sup>1</sup> –Glu <sup>20</sup>	Met <sup>1</sup>
c	Leu <sup>100</sup> –Glu <sup>124</sup>	
c*	Leu <sup>100</sup> –Glu <sup>124</sup>	Met <sup>122</sup>

**Table 2.** Receptor Binding Activity Obtained Using ELISA

Samples	Receptor binding activity (%)*			
	# 1	# 2	# 3	Average (n=3)
NS	105	103	98	102
HD	97	89	81	89
PD	91	75	84	83
FO	67	37	35	46

\*: Relative activity against G-CSF drug product (reference material).

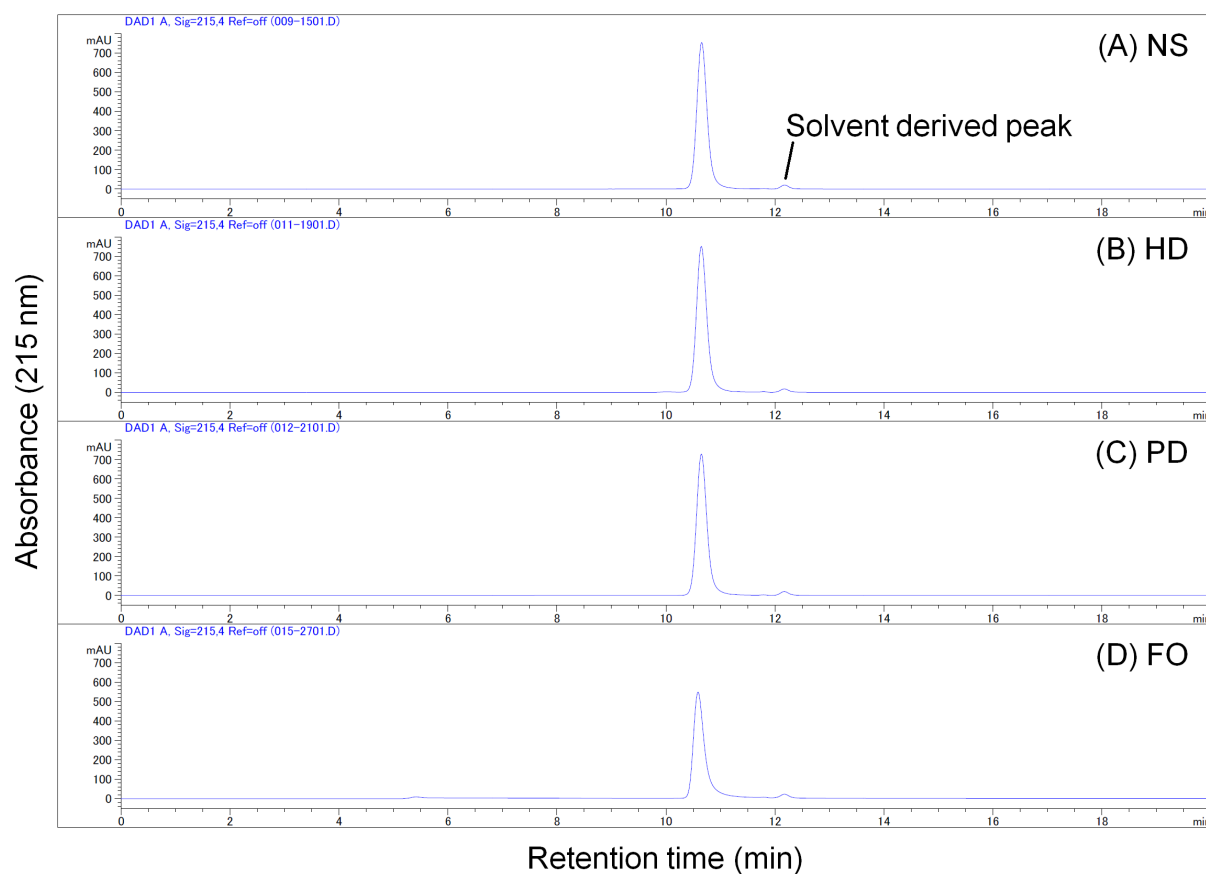


**Figure 1.** SEC chromatograms of the NS (a), HD (b), PD (c) and FO (d) samples. Only the main peak was clearly observed, and impurities such as aggregates did not appear in any chromatograms.



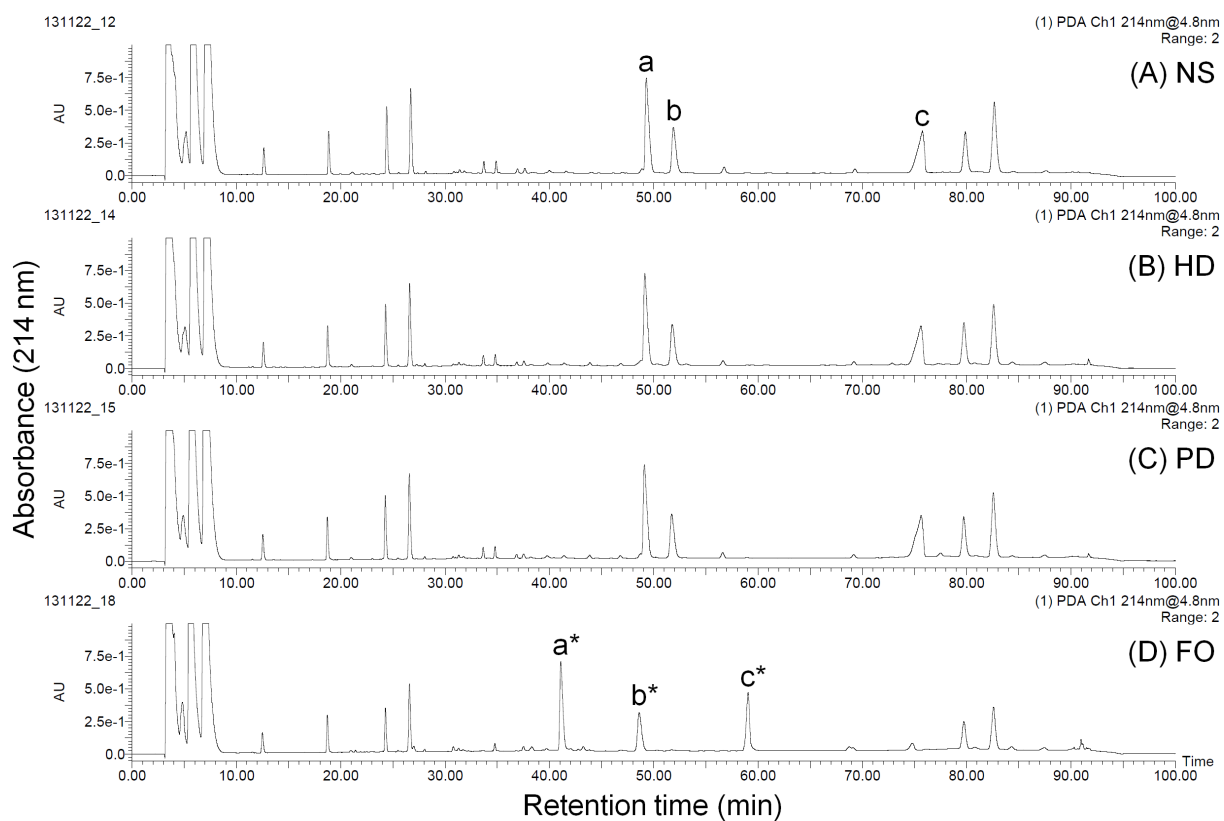


**Figure 2.** UV chromatograms of the peptides from the NS (a), HD (b), PD (c) and FO (d) samples, generated by Glu-C digestion. Only the FO sample showed the peak shifts corresponding to methionine oxidation. Details of the oxidized peptides are summarized in Table 1.

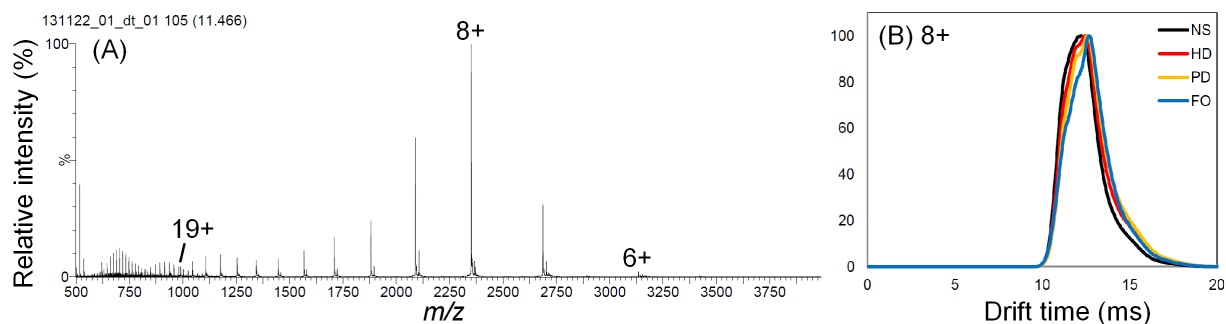


**Figure 3.** ESI mass spectrum of the NS sample (a) and driftgrams of 8+ charged ions of the stress-exposed and non-stressed G-CSF (b). Driftgrams of the NS, HD, PD and FO samples were overlaid with the color code described in the figure. The FO sample showed a slight delay in the peak in terms of the drift time.

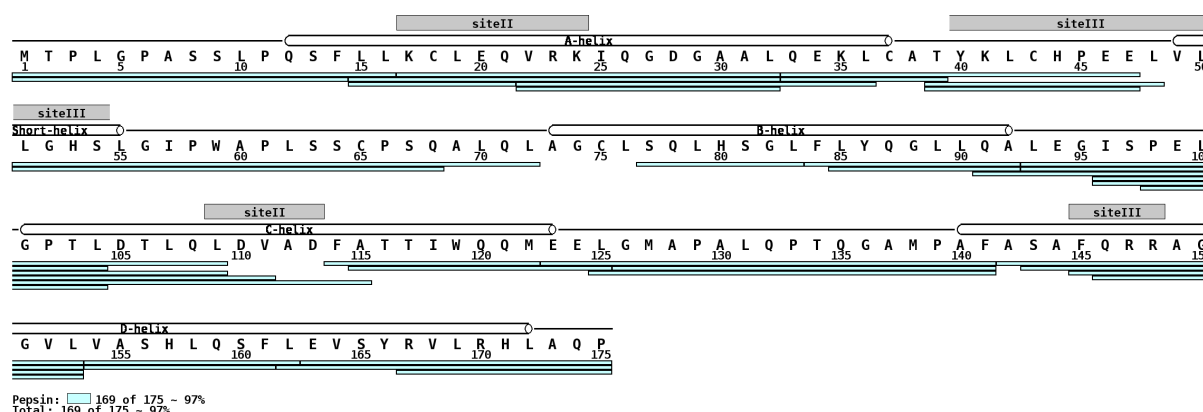


**Figure 4.** Peptic peptides of G-CSF identified by MS<sup>E</sup> experiments. Four receptor recognition sites (site II and site III) are indicated on the amino acid sequence of G-CSF [19] [PDB code 2D9Q]. The figure was drawn using the free software “MS tools” described in [30].

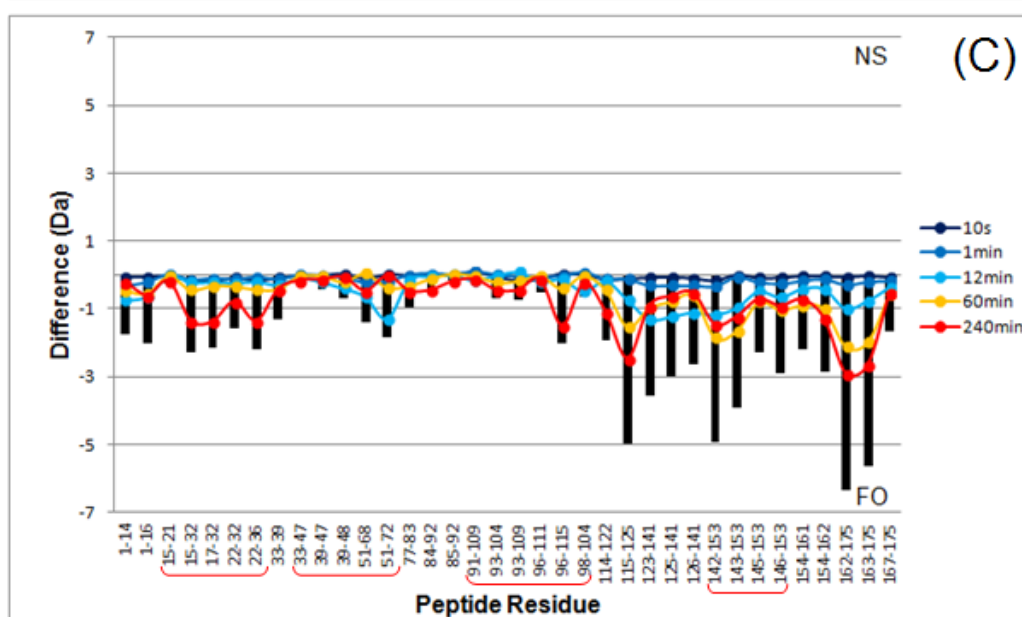
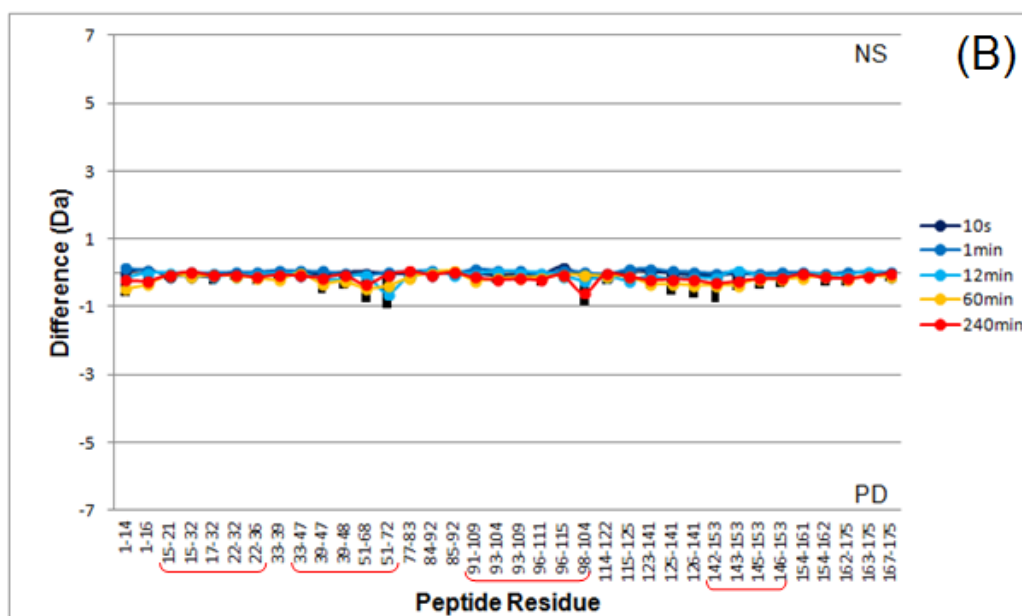
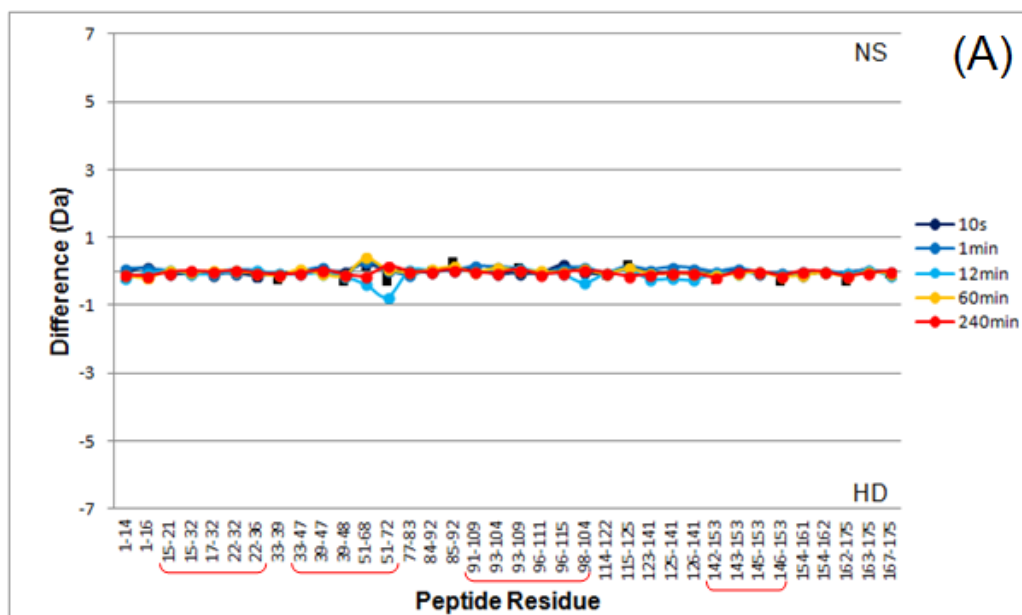


**Figure 5.** Difference-analysis charts (upper panel) of the HD (A), PD (B), and FO (C) samples (lower panel) compared with the NS sample, as obtained from the first trial of HDX-MS. The x-axis shows the common peptides of the two samples (red braces indicate the peptides that include receptor recognition sites), and the y-axis shows the mass difference calculated by subtraction of the observed mass value of the HD, PD, and FO samples from that of the NS sample. The vertical black bar shows the sum of each time point's mass difference. Based on the results, the FO sample shows a significant difference relative to NS; in particular, the N- and C-terminal regions including receptor recognition sites show a significant increase in deuterium uptake. This suggests that the higher-order structure of the FO sample is rather loosened, especially around both end regions. Similar results were obtained from the other two independent experiments.

## Supplemental Information

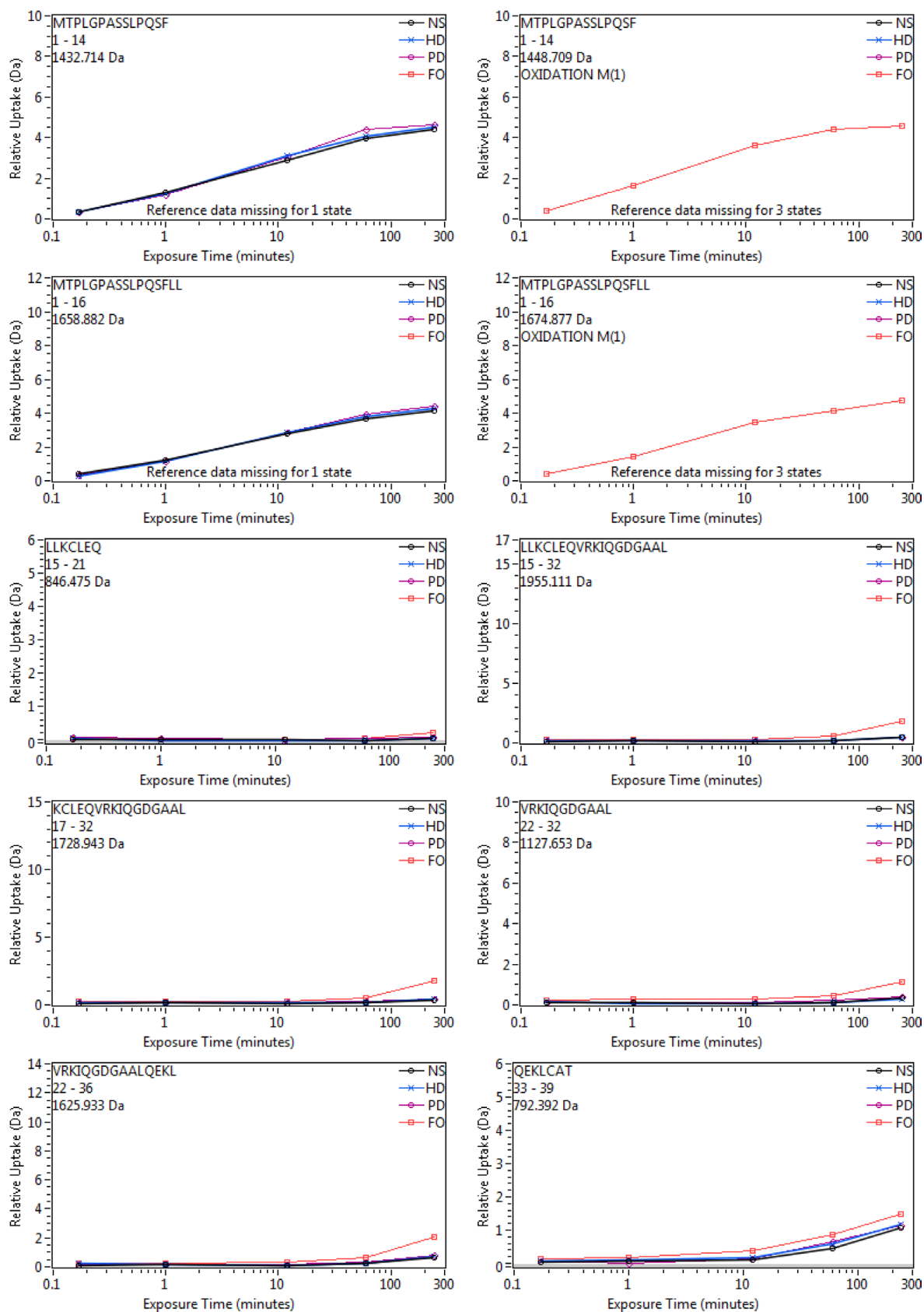


**Figure S-1.** Deuterium uptake curves of the peptides 1/5

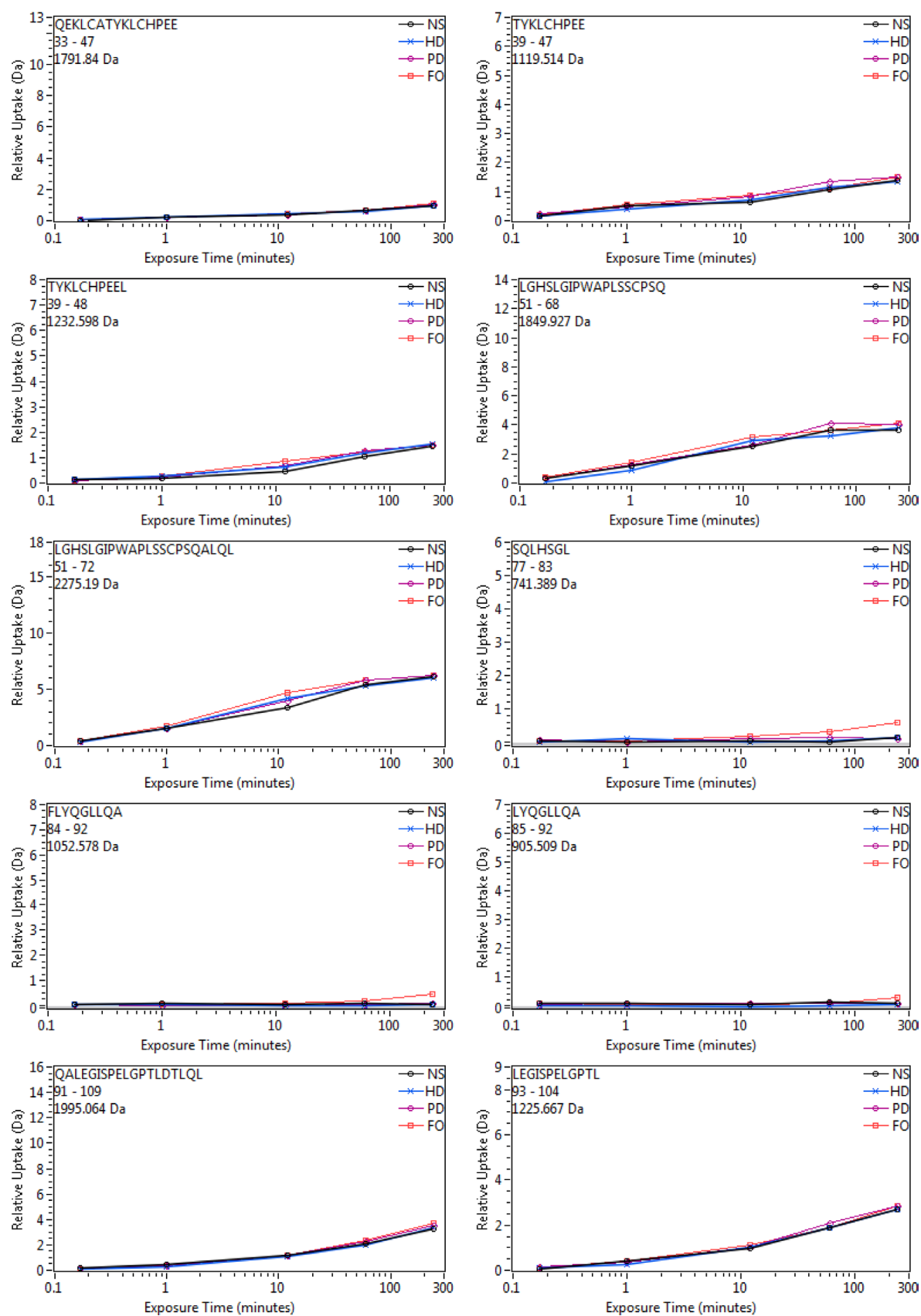


**Figure S-1.** Deuterium uptake curves of the peptides 2/5

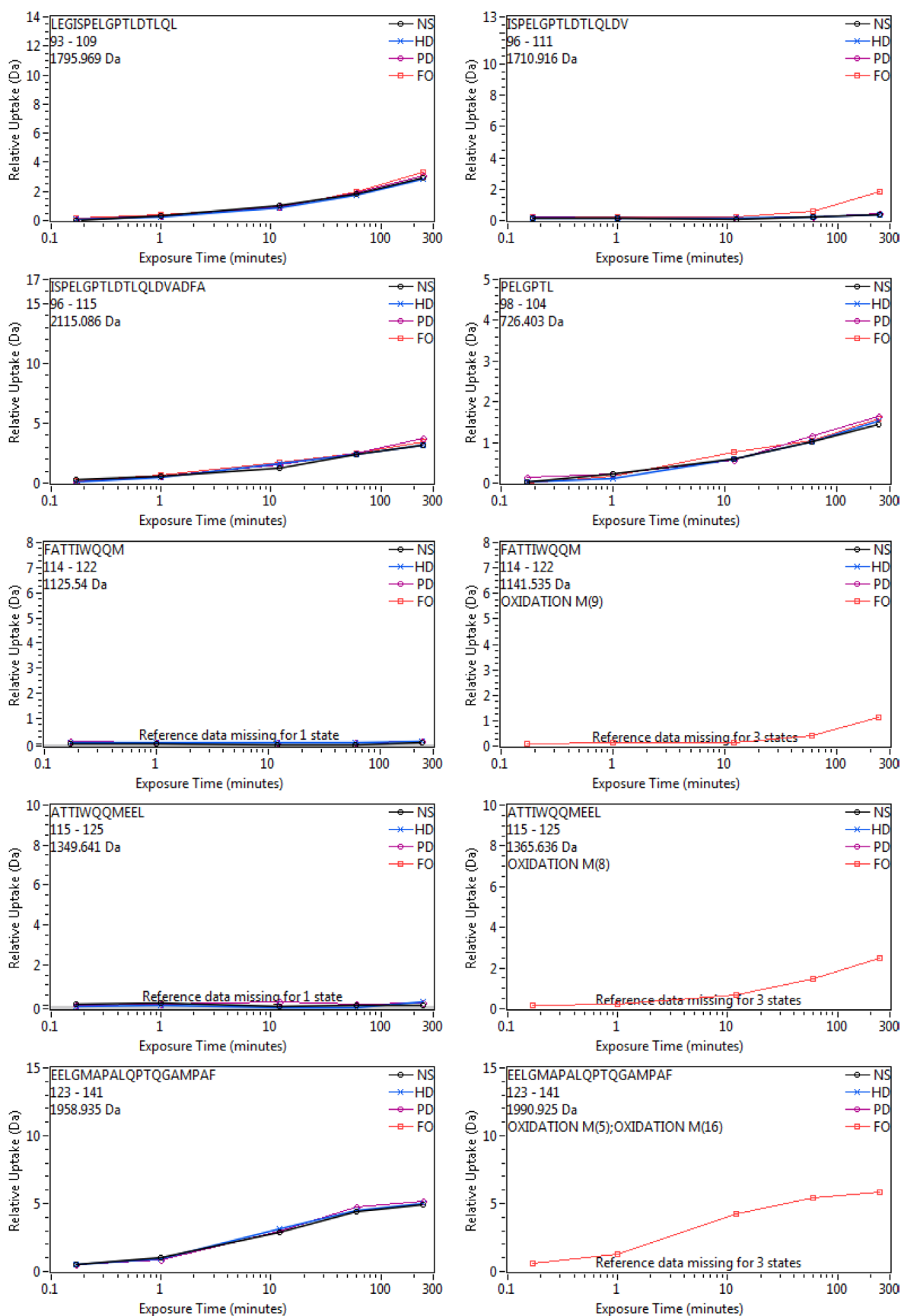


**Figure S-1.** Deuterium uptake curves of the peptides 3/5

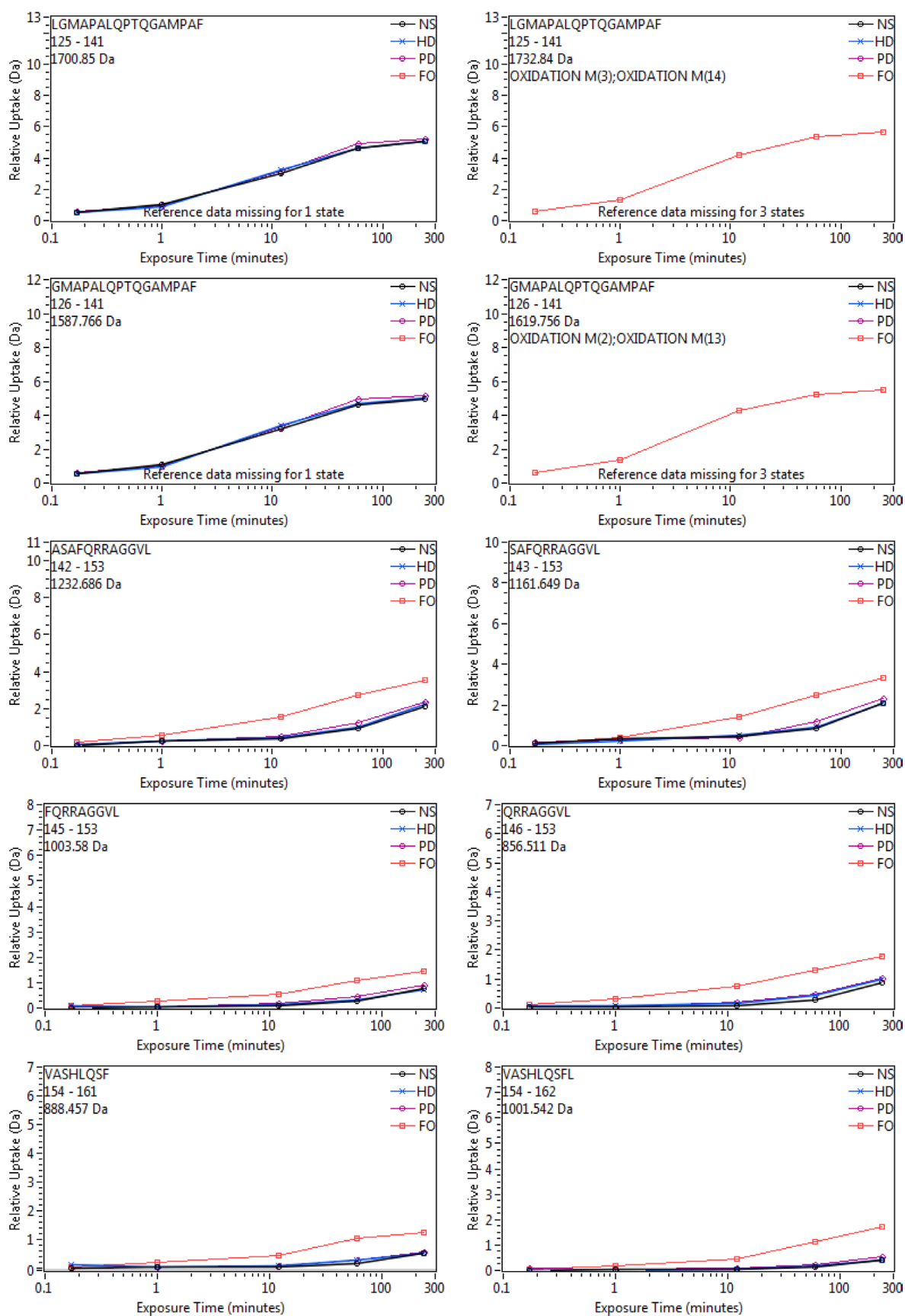


**Figure S-1.** Deuterium uptake curves of the peptides 4/5



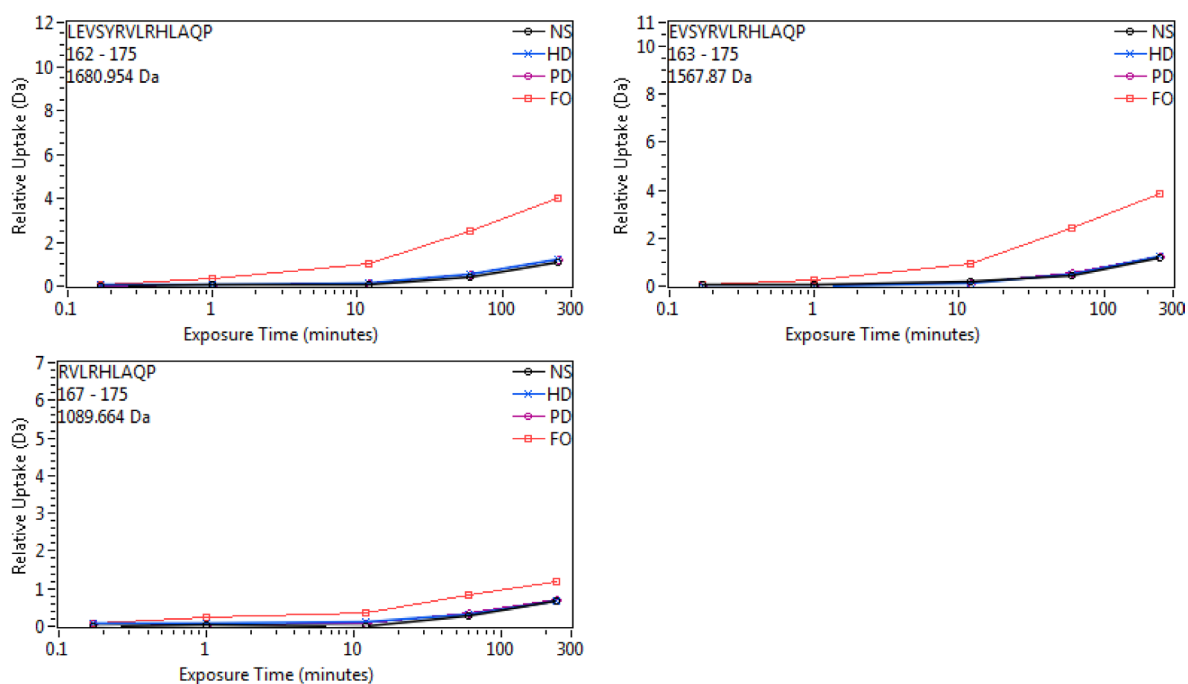


**Figure S-1.** Deuterium uptake curves of the peptides 5/5

Deuterium uptake transition from 10 s to 240 min are indicated for the first trial of HDX of the NS, HD, PD and FO samples.

Peptide sequence, position and monoisotopic molecular mass are shown in the upper left corner in each panel.

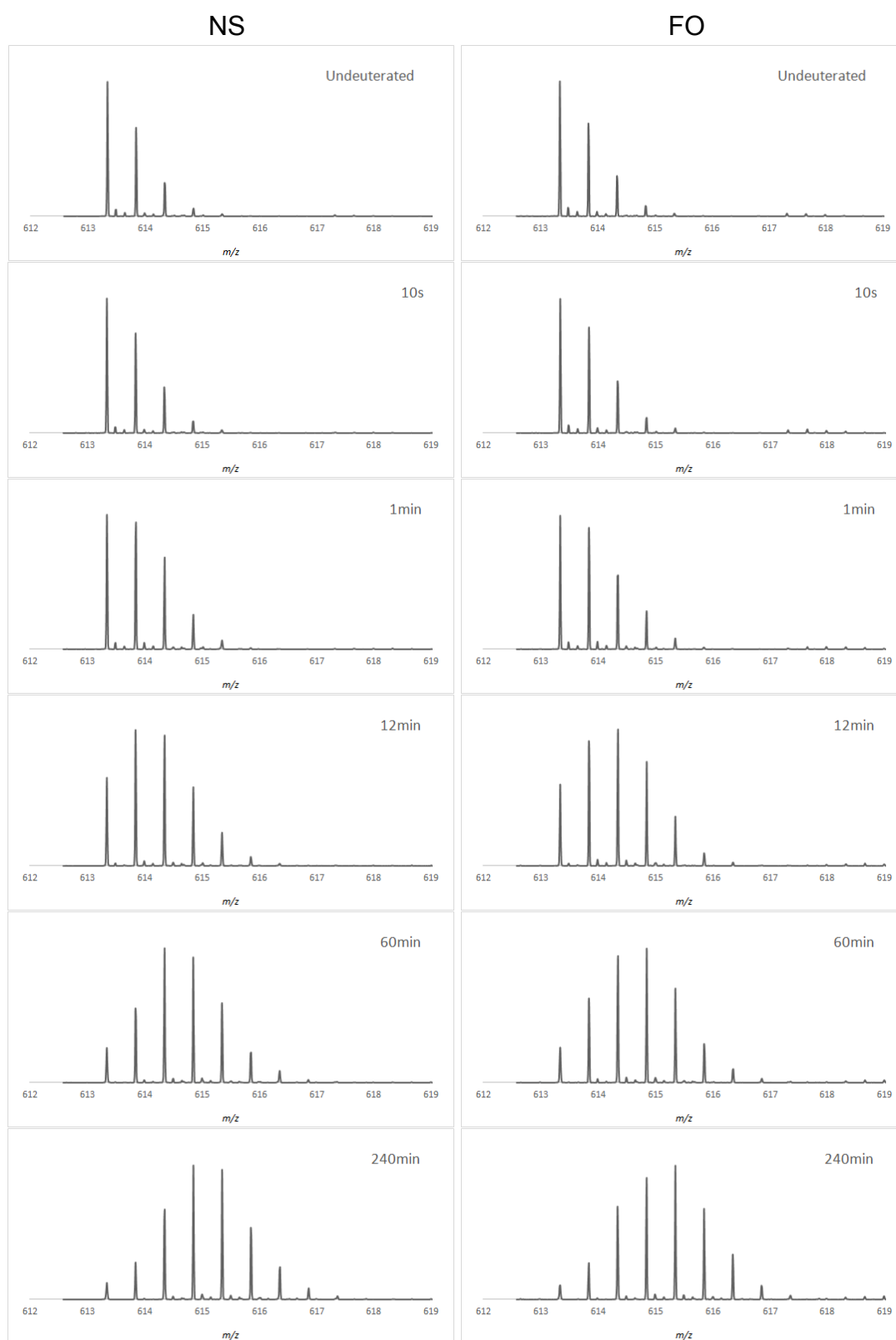


**Figure S-2.** Mass spectra of peptide 93-104 of the NS (left) and FO (right) samples

No significant difference was found between each two mass spectra.

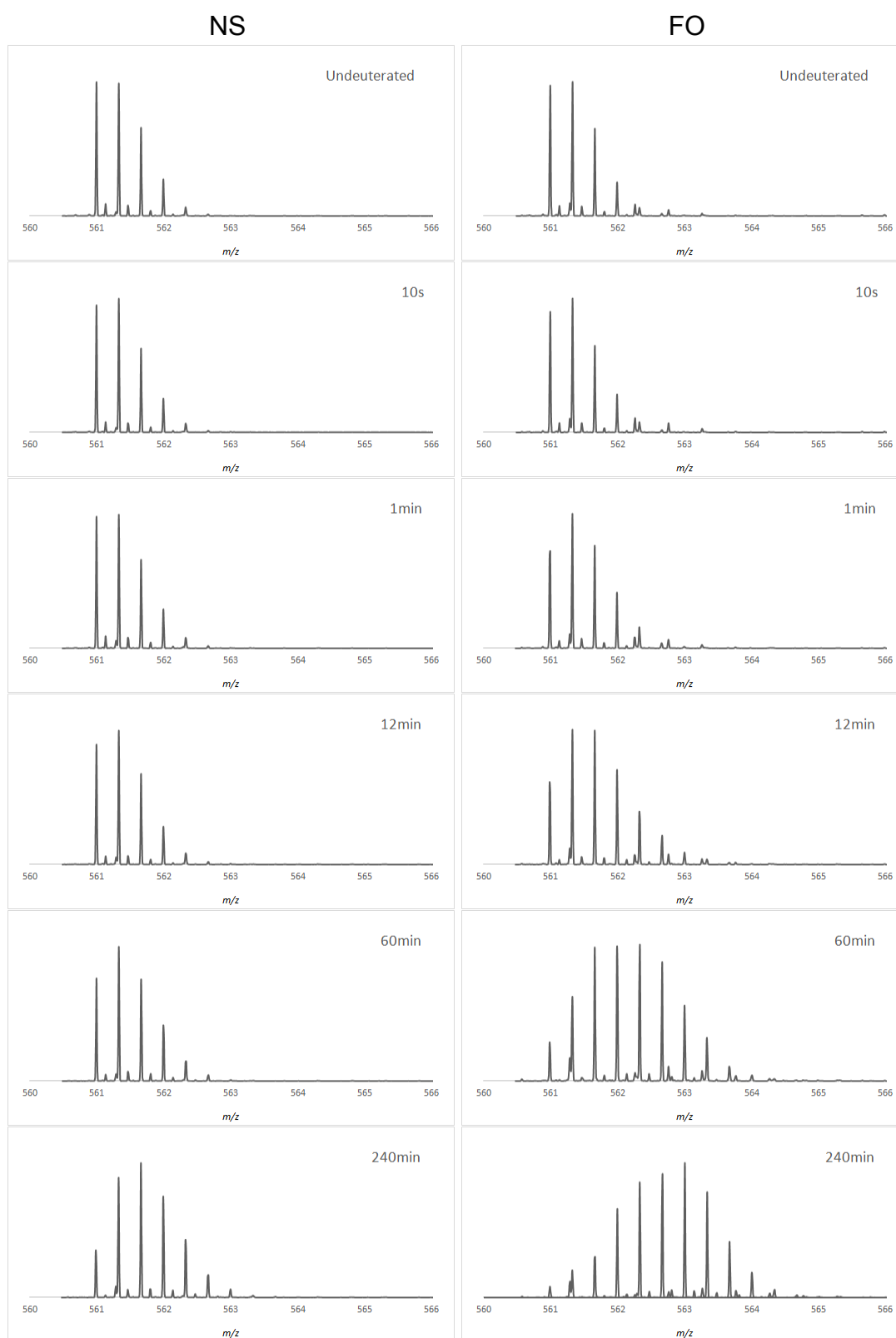


**Figure S-3.** Mass spectra of peptide 162-175 of the NS (left) and FO (right) samples

Peptide 162-175 of the FO sample demonstrated a larger mass increase than that of NS.